Allosteric interactions between GABA B1 subunits control orthosteric binding sites occupancy within GABA B oligomers

Gregory D Stewart, Laetitia Comps-Agrar, Lenea Blanc Nørskov-Lauritsen, Jean-Philippe Pin, Julie Kniazeff

Allosteric interactions between $GABA_{B1}$ subunits control orthosteric binding sites occupancy within $GABA_B$ oligomers

Gregory D. Stewart[1,3], Laëtitia Comps-Agrar[1,2,4], Lenea Blanc Nørskov-Lauritsen[1,5], Jean-Philippe Pin & Julie Kniazeff

[1] Institut de Génomique Fonctionnelle, CNRS, INSERM, Univ. Montpellier, France.
[2] Cisbio Bioassays, Codolet, France

Footnotes:
[3] Present address: Drug Discovery Biology, Monash Institute of Pharmaceutical Sciences, Parkville, VIC, Aust.

[4] Present address: Genentech, 1 DNA Way, South San Francisco, CA 94080, USA

[5] Present address: Novo Nordisk, Vandtårnsvej 108, DK-2860 Søborg, Denmark

Corresponding author : Julie Kniazeff, Institut de Génomique Fonctionnelle, 141 rue de la Cardonille, F-34094 Montpellier Cedex 5, France. Email : julie.kniazeff@igf.cnrs.fr

Highlights:

- Oligomeric association of $GABA_B$ receptor is altered by mutations in $GABA_{B1}$ VFT
- Destabilization of $GABA_B$ VFT oligomeric interface increases coupling efficacy
- The number of binding sites is increased by oligomer VFT interface destabilization
- $GABA_B$ receptor oligomerization promotes a negative allostery for ligand binding
- Oligomerization of the $GABA_B$ receptor offers new way to modulate its signaling

Abstract.

The $GABA_B$ receptor was the first G protein-coupled receptor identified as an obligate heterodimer. It is composed of two subunits, $GABA_{B1}$ containing the agonist binding site and $GABA_{B2}$ responsible for G protein activation. The $GABA_B$ receptor was found to associate into larger complexes through $GABA_{B1}$-$GABA_{B1}$ interactions, both in transfected cells and in brain membranes. Here we assessed the possible allosteric interactions between $GABA_B$ heterodimers by analyzing the effect of mutations located at the putative interface between the extracellular binding domains. These mutations decrease, but do not suppress, the Förster resonance energy transfer (FRET) signal measured between $GABA_{B1}$ subunits. Further analysis of one of these mutations revealed an increase in G protein coupling efficacy and in the maximal antagonist binding by approximately two-fold. Hypothesizing that a tetramer is an elementary unit within oligomers, additional FRET data using fluorescent ligands and tagged subunits suggest that adjacent binding sites within the $GABA_B$ oligomers are not simultaneously occupied. Our data reveal a strong negative cooperativity between $GABA_{B1}$ binding sites within $GABA_B$ oligomers. Accordingly, $GABA_B$ receptor assembly appears to limit receptor signaling to G proteins, a property that may offer novel regulatory mechanism for this important neuronal receptor.

Keywords:

G protein-coupled receptors; Oligomers; Allostery; GABA

1. Introduction.

γ-aminobutyric acid (GABA), the main inhibitory neurotransmitter in the adult central nervous system, limits neuronal excitability predominantly by inducing membrane hyperpolarization and reducing neurotransmitter release. The $GABA_B$ receptor is a G protein-coupled receptor (GPCR), broadly expressed in the brain and key player in GABAergic inhibition. It is known to inhibit Cav2 channels that controls neurotransmitter release at both excitatory and inhibitory presynaptic terminals; and to activate postsynaptic Kir3 channels in dendrites, promoting post-synaptic membrane hyperpolarization (Bettler et al., 2004; Ulrich and Bettler, 2007). Accordingly, the $GABA_B$ receptor plays a pivotal role in the modulation of many pathways throughout the brain (Bowery et al., 2002).

Preclinical studies using both, $GABA_B$ receptor agonists and antagonists, suggested that the $GABA_B$ receptor could be an attractive target for the development of therapeutics for many neurological disorders including alcoholism, addiction, anxiety or depression (Cryan and Kaupmann, 2005; Filip et al., 2015). However, only two agonist molecules are currently in the clinic: baclofen (Lioresal®), which is a muscle relaxant indicated for multiple sclerosis and currently under investigation for alcoholism treatment; and GHB (Xyrem®), a molecule to treat narcolepsy. The spectrum of therapeutic indications of these compounds is rather limited due to the associated side effects. To overcome this limitation, we would benefit from a more accurate knowledge of the mechanism of action of $GABA_B$ ligands.

The $GABA_B$ receptor belongs to the class C of the GPCR family together with the metabotropic glutamate receptors or the calcium sensing-receptor among others (Kniazeff et al., 2011). It is characterized by a large and structured extracellular domain called Venus Flytrap (VFT) and linked to a seven transmembrane core (7TM)

(Figure 1A). The $GABA_B$ receptor is an obligatory heterodimer, composed of the $GABA_{B1}$ and $GABA_{B2}$ subunits. $GABA_{B1}$ binds GABA in its VFT and $GABA_{B2}$ plays a major role in G protein activation (Galvez et al., 2001; Jones et al., 1998; Kaupmann et al., 1998; White et al., 1998). The heterodimers are stabilized by a coiled-coil interaction involving the intracellular C-termini as well as additional non-covalent interactions between their VFTs and 7TMs (Burmakina et al., 2014; Geng et al., 2013; Kammerer et al., 1999; Kuner et al., 1999). The coiled-coil interaction directly participates in a quality control of heterodimerization since $GABA_{B1}$ is retained in the endoplasmic reticulum (ER) unless the ER retention signal present in its C-terminus is masked through the coiled-coil interaction with $GABA_{B2}$ allowing the heterodimer to reach the plasma membrane (Calver et al., 2001; Margeta-Mitrovic et al., 2000; Pagano et al., 2001).

More recently, we and others reported that the $GABA_B$ receptor was associating into larger oligomeric entities (Calebiro et al., 2013; Comps-Agrar et al., 2011; Maurel et al., 2008). Indeed, when $GABA_B$ heterodimers were expressed at the cell surface, a significant lanthanide resonance energy transfer (LRET) was measured between two $GABA_{B1}$ subunits, indicating a direct interaction between $GABA_{B1}$ subunits from distinct heterodimers (Comps-Agrar et al., 2011; Maurel et al., 2008). This LRET was quantified using time resolved Förster resonance energy transfer (TR-FRET) measurement in which a delay is observed between light excitation and emission recording. In addition, by using single molecule microscopy, Calebiro et al. showed that even at low density, a large proportion of $GABA_B$ receptor tetramers could be detected. They also observed even larger entities when the receptor density increased (Calebiro et al., 2013). Furthermore, mass spectrometry analysis and TR-FRET measurements also support the existence of $GABA_B$ receptor oligomer in the

brain (Comps-Agrar et al., 2011; Schwenk et al., 2010). These findings give rise to important questions regarding the molecular and pharmacological transitions within the oligomers. In a previous study, the functional characterization of various oligomeric entities led us to propose a regulation of the G protein-coupling efficiency mediated by the $GABA_B$ receptor oligomerization. By using an engineered $GABA_{B1}$-like competitor (a $GABA_{B1}$ subunit deleted of its C-terminus and in which the GABA binding site is mutated) or by introducing mutations in $GABA_{B1}$ VFT (E380N + L382T), we measured a decrease in the oligomer TR-FRET signal which was correlated with an increased efficacy in G protein coupling as measured using the chimeric Gqi9 G protein, that forces Gi-coupled receptors to activate the phospholipase C (PLC) pathway (Comps-Agrar et al., 2011). These data suggest that the G protein signaling is restrained by the oligomerization of the $GABA_B$ receptor heterodimers through an unknown molecular mechanism.

In the present study, we aimed at better understanding the properties of the $GABA_B$ receptor oligomers by conducting further characterization of a $GABA_{B1}$ VFT mutant. We show that mutations at the VFT interface altered the oligomeric organization without preventing it, since oligomers can still be detected. Using one of the mutants, we show that mutating the VFT interface largely increases coupling efficacy to natural signaling of the $GABA_B$ receptor independently of any change in the agonist or antagonist affinity. This mutant also results in an approximately 2 fold increase in the number of binding sites. With additional LRET analysis of ligand interaction, our data reveal a strong negative allostery between binding sites within the oligomer such that not all $GABA_{B1}$ VFT can simultaneously bind a ligand in the oligomers. We propose that the $GABA_{B1}$ VFT interaction within the oligomers

promotes allosteric interactions between the VFTs that likely limit the number of active heterodimers in the oligomer to one per tetrameric unit.

2. Materials and Methods.

2.1. Chemicals:

Unless stated otherwise, compounds were purchased from Sigma Aldrich (St Quentin Fallavier, France).

2.2 Plasmids:

cDNAs encoding the $GABA_B$ subunits or mGlu2 with various tags (HA, cMyc, Flag or ST) and mutations were cloned in pRK5 plasmid and described previously (Doumazane et al., 2011; Maurel et al., 2008). Plasmid encoding cAMP EPAC sensor was obtained from Dr Lily Jiang (University of Texas Southwestern, Dallas).

2.3 Cell culture and transfection:

Human embryonic kidney (HEK293) cells (ATCC® CRL-1573™, Molsheim, France) were cultured in Dulbecco's Modified Eagle Medium (DMEM) (Life Technology, Cergy Pontoise, France) supplemented with 10 % fetal bovine serum (Sigma Aldrich) at 37 °C under 5 % CO_2. The cells were regularly tested and were mycoplasm-free (MycoAlert, Lonza, Levallois, France).

Cells were transiently transfected either by electroporation as previously described (Maurel et al., 2004) or using lipofectamine 2000 (Life Technology) using the manufacturer instructions. Following transfection, cells were seeded out either in 96-well microplates or 10 cm dishes and cultured for 24 h.

2.4 TR-FRET determination between ST-fused receptors

Cell surface receptors fused to a Snap-Tag (ST) were labeled using the non-cell-permeant fluorescent substrates: SNAP-Lumi4Tb and SNAP-Red in Tag-Lite buffer (Cisbio bioassays, Codolet, France) at 37 °C for 1 h. For TR-FRET measurement, the optimal concentrations were 100 nM of SNAP-Lumi4Tb and 600 nM of SNAP-Red. After 3 washes in Krebs buffer (10 mM Hepes pH 7.4, 146 mM NaCl, 4.2 mM KCl, 1 mM $CaCl_2$, 0.5 mM $MgCl_2$, 5.6 mM glucose, bovine serum albumin 0.1%), fluorescence was measured in a RUBYstar plate reader (BMG Labtech, Champigny sur Marne, France) using the following excitation – detection parameters: laser excitation 337 nm – 20 flashes; donor detection: 620 nm; acceptor detection: 665 nm. TR-FRET parameters delay: 50 µs; integration time: 400 µs. TR-FRET is calculated as the TR-FRET intensity, where the non-specific LRET due to random collisions and the contamination of the donor at the TR-FRET wavelength (665 nm) are subtracted. TR-FRET intensity = (signal at 665 nm measured on cells co-labeled with the donor and the acceptor) – (signal recorded on the same transfection labeled with the donor in absence of acceptor).

2.5 Cell surface expression determination by ST labeling

Cells from the same transfection as for the TR-FRET measurement were labeled at a saturating concentration of 300 nM SNAP-Lumi4Tb in Tag-Lite buffer at 37 °C for 1 h. After 3 washes in Krebs buffer, fluorescence was measured in a RUBYstar plate reader using the same parameters as for the TR-FRET measurement. Cell surface expression levels were calculated as the difference between the signal recorded at 620 nm on cells expressing the receptor and the signal recorded at 620 nm on mock transfected cells incubated with SNAP-Lumi4Tb.

2.6 Co-immunoprecipitation

Cells were transfected by electroporation (described above) with a 50:50 mix of HA-GB1 and Flag-GB1 co-expressed with cMyc-GB2, and seeded into 100 mm cell culture dishes. 24 h post-transfection cells were washed in ice-cold PBS then harvested in ice-cold lysis buffer (HEPES, 5 mM; NaCl 300 mM; NP-40, 20% v/v; glycerol, 9% v/v; dodecyl maltoside, 0.4% w/v, Roche protease inhibitor cocktail, 1 tablet); lysates were centrifuged to remove the nuclear fraction and a sample was assayed for protein content (BCA reaction, ThermoFisher). Samples were separated for input (5 µg) and immunoprecipitation (IP) (10 µg). Samples for IP were pre-cleared with Protein G agarose beads and then probed under gentle agitation for 16 h at 4 ºC with anti-Flag antibody-conjugated agarose beads, the samples for input were kept under the same conditions in the absence of agarose beads. After incubation the IP samples were centrifuged at low speed and washed three times in ice-cold lysis buffer. After the third wash the beads were resuspended into 4x SDS sample buffer (200 mM Tris-Cl (pH 6.8), 8% SDS (sodium dodecyl sulfate), 0.4% Bromophenol blue, 40% glycerol), as were the input samples. Samples were run on NuPage 3-8% Tris acetate gels (ThermoFisher) and subsequently transferred to PVDF membranes, blocked and probed with primary antibody (rabbit anti-HA or mouse anti-Flag, 1:1000) 16 h at 4 ºC; after washing, membranes were probed with secondary antibody (anti-mouse- or anti-rabbit-HRP) 60 min at room temperature, washed, then detected using Pierce SuperSignal Pico kit (ThermoFisher) and Amersham Hyperfilm (GE Life sciences).

2.7 Determination of cAMP production by bioluminescence resonance energy transfer (BRET)

Cells were transfected with the indicated receptor subunits and with BRET Epac (cAMP) sensor, Camyel (Jiang et al., 2007). 24 h post-transfection cells were washed in Assay buffer (150 mM NaCl, 2.6 mM KCl, 1.2 mM MgCl2, 10 mM dextrose, 10 mM HEPES, 2.2 mM CaCl2, 0.5%(w/v) bovine serum albumin, pH 7.4) and replaced with fresh assay buffer. Coelentrazine H (ThermoFisher) was added to each well for 5 min, 10 µM forskolin for 5 min and GABA for 10 min. The BRET signal was recorded at that time point (10 min after GABA addition) using a Mithras LB940 plate reader (Berthold, Thoiry, France) at 485 nm (Renilla Luciferase) and 530 nm (YFP). The BRET signal was expressed as the ratio of the signal at 530 nM divided by the signal at 485 nM and normalized to the wild-type response (no GABA = 0 %; 1 mM GABA = 100 %).

2.8 CGP54626-Red fluorescence binding experiments

For saturation binding experiments, cells transfected with the indicated receptor subunits were placed at 4 °C and washed twice with ice-cold Tris Krebs buffer (20 mM Tris, 118 mM NaCl, 1.2 mM KH_2PO_4, 1.2 mM $MgSO_4$, 4.7 mM KCl, 1.8 mM $CaCl_2$, pH 7.4). The cells were then incubated with increasing concentrations of the fluorescently labeled antagonist, DY647-CGP54626 (CGP54626-Red; 0-30 nM) for 3 h at 4 °C. Non-specific binding was determined for each concentration in the presence of 1 mM GABA. The cells were then washed three times quickly with ice-cold Tris Krebs buffer to remove the unbound ligand.

Competition binding experiments were performed using increasing concentrations of GABA or CGP54626 in the presence of K_D concentration of CGP54626-Red (Cisbio), 10µM non-labeled CGP54626 (Tocris) was used to determine non-specific binding.

The fluorescence was immediately measured using an Infinite F500 plate reader (Tecan, Lyon, France) using a xenon lamp excitation at 610 nm (10 flashes) and a detection wavelength at 670 nm over 1 ms. The signal was expressed as the difference of fluorescence signal at 670 nm between CGP54626-Red and CGP54626-Red in the presence of GABA.

2.9 Cell surface ELISA

Cell surface ELISA has been performed us previously described (Maurel et al., 2008) using HA-tagged $GABA_{B1}$ subunits (wild-type or mutant) and the HRP-conjugated anti-HA clone 3F10 from Roche (Sigma).

2.10 TR-FRET and fluorescence measurements using fluorescent antagonists

Cells transfected with the $GABA_B$ subunits were washed twice with ice-cold Tris Krebs buffer and then incubated at 4 °C for 3 h with 10 nM CGP54626-Lumi4Tb and increasing concentrations of CGP54626-Red. After 3 quick washes with ice-cold Tris Krebs buffer to remove unbound ligands, TR-FRET and fluorescence signal were recorded immediately using both a RUBYstar (TR-FRET, 620 nm) and an Infinite F500 (670 nm) plate readers using the parameters indicated in the previous sections. Unspecific binding was assessed using 1 mM GABA and subtracted from the signal.

2.11 Data analysis

Data were analyzed using the GraphPad software (San Diego, CA, USA).

2.11.1 For saturation fluorescence binding data, non-specific and total binding data were fitted according to the following equation.

$$Y = \frac{B_{max} \cdot [\mathrm{A}]}{[\mathrm{A}] + K_{\mathrm{A}}} + \mathrm{NS} \cdot [\mathrm{A}]$$

where Y is the fluorescence binding, B_{max} is the total receptor density, [A] is the fluorescent ligand concentration, K_A is the equilibrium dissociation constant of CGP54626-Red, and NS is the fraction of non-specific fluorescence binding.

2.11.2 Competition binding data were fitted with a one-site binding equation to analyze specific binding of each ligand:

$$Y = \frac{(\text{Top} - \text{Bottom})}{1 + 10^{(\log [I] - \log \text{IC}_{50})}} + Bottom$$

where Y represents the percentage of specific binding; Top and Bottom denote the maximal and minimal asymptotes of the curve, respectively; [I] is the concentration of inhibitor; and IC_{50} is the concentration of competitor that produces half the maximal response.

2.11.3 Concentration-response data generated from cAMP inhibition assays were fitted according to the following three-parameter logistic equation:

$$E = \text{basal} + \frac{\text{E}_{\text{max}} - \text{basal}}{1 + 10^{(-\text{pEC}_{50} - [\text{A}])}}$$

where E is effect, E_{max} and basal are the top and bottom asymptotes of the curve, respectively, [A] is the agonist concentration, and pEC_{50} is the negative logarithm of the agonist concentration that gives a response halfway between E_{max} and basal.

3. Results.

3.1 Alteration of $GABA_B$ oligomeric organization by mutating $GABA_{B1}$ VFT.

Based on the analysis of the VFT-containing tetrameric AMPA receptor GluR2 crystal structure (Sobolevsky et al., 2009), we previously proposed a patch of residues within $GABA_{B1}$ VFT likely involved in the $GABA_B$ receptor oligomerization interface (Comps-Agrar et al., 2011). We confirmed these observations here using previously reported and novel mutants, all located in the same region in the $GABA_{B1}$ VFT (E380N + L382T; T410N + E412T; E413N) (Figure 1B). We used N-terminal SNAP-tagged (ST) version of $GABA_{B1}$ that can be labelled specifically at the cell surface using non cell-permeant SNAP substrates, SNAP-Lumi4Tb or SNAP-Red, compatible with LRET (Figure 1A). HEK293 cells were transfected with $GABA_{B2}$ and with increasing concentrations of $GABA_{B1}$ wild-type or mutant. After labeling with an optimized ratio of SNAP-Lumi4Tb and SNAP-Red, the TR-FRET signal was recorded. In parallel, the cell surface expression of $GABA_B$ heterodimers was determined by labeling ST at a saturating concentration of SNAP-Lumi4Tb. Although all the mutations decreased the TR-FRET signal measured between $GABA_{B1}$ subunits at any cell surface expression, none of them suppressed the TR-FRET signal (Figure 1C). Compared to the low TR-FRET signal recorded between ST-$GABA_{B2}$ subunits that do not directly interact, the signal recorded when using the mutated ST-$GABA_{B1}$ subunits was higher (Figure 1C). This suggests that the mutated heterodimers are still in proximity and likely interacting but the mean distance between their $GABA_{B1}$ VFT is increased.

We then further analyzed one of these mutants, that carrying both the E380N and L382T (this mutant $GABA_{B1}$-N380/T382 will be referred to as $GABA_{B1}$-NT) by

performing co-immunoprecipitation experiments. We co-expressed in HEK293 cells both HA and Flag-tagged $GABA_{B1}$ wild-type or $GABA_{B1}$-NT together with $GABA_{B2}$ and performed an anti-Flag immunoprecipitation followed by an anti-HA immunoblot (Figure 1D). In agreement with the remaining TR-FRET signal, the heterodimers containing $GABA_{B1}$-NT could still be co-immunoprecipitated (Figure 1D). As a negative control, we used HA-mGlu2 homodimers that could not be immunoprecipitated by Flag-$GABA_B$ heterodimer. These co-immunoprecipitation experiments suggest that the $GABA_{B1}$-NT mutation is not sufficient to prevent the interaction between $GABA_B$ heterodimers. Altogether, our data indicate that the NT mutation in $GABA_{B1}$ very likely disturbs the $GABA_{B1}$ VFTs interaction within the oligomer, thus decreasing probably the affinity between the $GABA_B$ receptors.

3.2 $GABA_B$ receptor oligomerization reduces native Gi protein coupling efficiency

We then characterized further the pharmacological consequences of the oligomer destabilization induced by the N380+T382 mutation in $GABA_{B1}$. We first assessed the effect of the mutation on G protein activation. The $GABA_B$ receptor is endogenously coupled to Gi/o protein family, which inhibits adenylyl cyclase activity, hence decreasing cAMP level (Bowery et al., 2002). Here, we used the cAMP CAMYEL sensor to directly monitor cAMP level in transfected cells (Figure 2A). It is a BRET sensor that changes conformation upon cAMP binding: in the absence of cAMP, the BRET signal is high and in the presence of cAMP, the signal decreases (Jiang et al., 2007). HEK293 cells were transfected with CAMYEL and with either the wild-type or the NT mutant receptor. An initial cAMP production was induced by

forskolin addition before stimulating the receptor with increasing concentrations of GABA. As expected, the BRET signal increased in the presence of GABA since it reduced cAMP level (Figure 2B). When comparing the signals obtained using the wild-type $GABA_{B1}$ or $GABA_{B1}$-NT, the GABA potency was similar for both conditions (wild-type: pEC50 = 5.80 ± 0.12; NT: pEC50 = 5.91 ± 0.39), while the maximal response was higher for $GABA_{B1}$-NT (182 ± 24 % of wild-type response) despite a similar cell surface expression (107 ± 13 % of wild-type expression as determined by ELISA). This indicates that the efficacy of G protein response is tightly regulated by the oligomerization of the $GABA_B$ receptor. This observation is in line with our previous study using the Gqi9 chimeric G protein that allows Gi coupled receptor to stimulate phospholipase C (Comps-Agrar et al., 2011). Taken together, these various observations support that $GABA_{B1}$-NT is proven to be useful in elucidating the properties of the $GABA_B$ receptor oligomers.

3.3 $GABA_B$ receptor oligomerization alters the orthosteric ligand binding properties

We hypothesized that the limitation of the coupling efficacy in oligomers was related to negative allosteric transitions between heterodimers within the oligomers. To verify this, we analyzed the ligand binding properties of the wild-type and mutated oligomers as allosteric transitions within GPCR oligomers may reflect on the apparent binding affinity. We first performed a competitive binding assay to compare the affinity of GABA, the endogenous agonist, and of CGP54626, an orthosteric antagonist with inverse agonist properties, for the intact versus the destabilized $GABA_B$ oligomers. We transfected cells with the vectors encoding the wild-type or the NT mutant $GABA_B$ receptors and carried out cell surface competition binding experiments using the non-permeant fluorescent antagonist (CGP 54626-Red) as a

tracer (Figure 3A). When displacing the tracer with the unlabeled CGP54626, the IC_{50} was similar for both combinations (wild-type: pIC_{50} = 8.88 ± 0.14; NT: pIC_{50} = 8.90 ± 0.21). Similarly, GABA IC_{50} value was not altered when introducing the mutation that destabilized the oligomer (wild-type: pIC_{50} = 5.12 ± 0.10; NT: pIC_{50} = 5.09 ± 0.12). These data indicate that the apparent affinity of the ligands was not modified when destabilizing the oligomers.

Using the fluorescent antagonist, we also performed saturation binding experiments on cells expressing either the wild-type or the N380 + T382 $GABA_B$ receptor to better characterize the binding properties of the different oligomeric states. We ensured that we had a similar cell surface expression of the receptor between the two conditions (wild-type: $2.16x10^6$ ± 0.07 $x10^6$ RLU; NT: $2.41x10^6$ ± 0.07 $x10^6$ RLU in cell surface ELISA (Figure 3B)). The K_D was similar in both conditions (wild-type: K_D = 4.72 ± 1.08 nM; NT: K_D = 2.63 ± 0.61 nM). However, the B_{max} was surprisingly about twice higher when using $GABA_{B1}$-NT (wild-type: B_{max} = 5660 ± 410 RFU; NT: B_{max} = 9022 ± 632 RFU) (Figure 3C). This indicates that the apparent number of CGP54626 binding sites at the equilibrium was approximately twice higher in destabilized oligomers than in wild-type oligomers. This suggests that only parts of the binding sites are simultaneously occupied in the oligomers and the destabilization of the VFT interaction results in an increase in the number of occupied binding sites. Altogether, these observations suggest a strong negative cooperativity between orthosteric binding sites within the oligomers preventing the simultaneous occupancy of all sites.

3.4 No LRET is detected between adjacent binding sites within the $GABA_B$ oligomer.

We decided to address the proposed negative allostery between binding sites by taking advantage of CGP54626 derivatized with the LRET compatible fluorophores Lumi4Tb and Red. Previously, we showed that $GABA_{B1}$ subunits were in close proximity within the oligomers as evidenced by the high TR-FRET signal measured between ST fused to $GABA_{B1}$ VFT (Figure 1A). We could thus reasonably hypothesize that the simultaneous binding of CGP54626-Lumi4Tb and CGP54626-Red to orthosteric binding sites, located within $GABA_{B1}$ VFTs would give rise to a significant TR-FRET signal. HEK293 cells were transiently transfected with vectors encoding $GABA_B$ receptor and incubated with 10 nM CGP54626-Lumi4Tb (twice the Kd of the fluorescent antagonist) and increasing concentrations of CGP54626-Red. After washes, the amounts of CGP54626-Lumi4Tb and CGP54626-Red bound to the cells were quantified by direct measurement of the fluorescence of each fluorophore at their respective wavelength, and subsequently the TR-FRET signal was also measured. We observed that the more Red antagonist was added, the less Lumi4Tb was bound to the cells, which is in line with a competition between the two fluorescent antagonists (Figure 4A). Moreover, the two curves cross at 50% of maximal binding indicating a site-occupancy with 50% LRET donor antagonists and 50% LRET acceptor antagonists, which are optimal conditions for LRET to occur. Surprisingly, we did not observe the expected TR-FRET bell-shape curve, with the maximal signal obtained for an equi-binding of the two fluorescent antagonists, as previously shown for TR-FRET between ST (Maurel et al., 2008). Instead, we obtained a sigmoidal curve that resembled that of Lumi4Tb fluorescence (Figure 4B). In addition, the signal recorded was very weak, which rather suggests a bleed-through of Lumi4Tb emission into the TR-FRET channel and supports an absence of actual LRET between fluorescently derivatized antagonists within the $GABA_B$ oligomers.

To determine the impact of the derivatization of CGP54626 with the fluorophores on the photo-physical properties of the chromophores, we tested whether a TR-FRET signal could be recorded between a ST fused at the N-terminus of $GABA_{B1}$ or $GABA_{B2}$ and the fluorescent CGP54626 bound to $GABA_{B1}$. We obtained a significant TR-FRET signal on cells transfected with ST-$GABA_{B1}$ and $GABA_{B2}$ and labeled with CGP54626-Lumi4Tb and SNAP-Red and conversely with CGP54626-Red and SNAP-Lumi4Tb (data not shown), confirming that the fluorescent antagonists are suitable for LRET studies even after binding to $GABA_{B1}$ VFT. In addition, we verified that the CGP54626 moiety was still able to bind to $GABA_{B1}$ with a high affinity (4.98 and 4.91 nM for CGP54626-Lumi4Tb and CGP-54626-Red, respectively).

We then directly compared the different TR-FRET signals that could be measured within the $GABA_B$ oligomer using ST and fluorescent antagonist labeling. Indeed, by transfecting HEK293 cells with vectors encoding ST-$GABA_B$ receptor, we could study three different LRET combinations: the LRET between two ST; the LRET between the ST and the antagonist; and the LRET between two antagonists. Cells from the same transfection could be labeled with each combination of fluorescent ligands and substrates and therefore all the resulting TR-FRET measurements could be directly compared (Figure 4C). When the ST was fused to $GABA_{B2}$, the TR-FRET signal between ST was low as previously shown (Figure 1). A high TR-FRET signal was measured between CGP54626-Lumi4Tb and SNAP-Red and this signal was even higher when ST was fused to the $GABA_{B1}$ subunit. This is coherent with a shorter distance between the antagonist, bound to $GABA_{B1}$ VFT, and the ST fused to $GABA_{B1}$ rather than fused to $GABA_{B2}$. When using a combination of CGP54626-Lumi4Tb and CGP54626-Red, no significant TR-FRET signal could be

detected independently of the ST fusion used. This result suggests that two consecutive binding sites are unlikely to be occupied at the same time within the oligomer and further supports the existence of a negative allostery between adjacent $GABA_{B1}$ binding sites. Of note, when using $GABA_{B1}$-NT and $GABA_{B2}$, we could not detect any TR-FRET signal between antagonists either (Supplementary Figure 1). Such finding may appear surprising when considering the increase in apparent number of binding sites thus the number of bond antagonists at the equilibrium. However, it is possible that the destabilization of the VFT association resulting from the N380+T382 mutation increases the mean distance between two $GABA_{B1}$ binding sites such that these are too distant for an efficient LRET to occur.

4. Discussion.

The discovery that the $GABA_B$ receptor was an obligatory heterodimer was a breakthrough in the GPCR field, highlighting the possibility that other GPCRs may also associate in heterodimeric entities. More recently, $GABA_B$ receptor heterodimers were shown to associate into larger entities, both in transfected cells and in the brain (Calebiro et al., 2013; Comps-Agrar et al., 2011; Maurel et al., 2008; Schwenk et al., 2010), raising questions regarding the significance, the properties and the structural organization of such complexes. Here we characterized a mutant that destabilizes the oligomer interface at the level of the VFT. This is well illustrated by a decrease in the TR-FRET signal between $GABA_{B1}$ VFTs. In this mutant the allosteric interactions between the $GABA_B$ receptors within the oligomers are prevented as shown by the increase of both the G protein signaling efficacy and the number of binding sites. Further LRET studies between ligands, and between the ligand and the subunits are consistent with a decrease of occupied binding sites in the oligomer down to a single ligand bound per $GABA_B$ tetrameric unit, despite the presence of two identical binding sites. Taken together our data revealed a strong negative allostery between the $GABA_{B1}$ VFTs within the oligomer.

Although a direct interaction between the $GABA_{B1}$ subunits of the heterodimer is essential for the formation of larger $GABA_B$ complexes, the precise molecular organization of the oligomer is still unknown. We have previously reported that the $GABA_{B1}$ VFT plays a critical role in the formation of the oligomers (Comps-Agrar et al., 2011). In the tetrameric ionotropic glutamate receptors (iGluRs), the amino-terminal extracellular domain of each subunit is a VFT similar to those of $GABA_B$ subunits. Several high resolution structures of iGluRs were solved revealing two main

possibilities for two VFT dimers to interact (Herguedas et al., 2016; Lee et al., 2014; Sobolevsky et al., 2009; Zhu et al., 2016). A first arrangement involves a small area of the C-terminal lobes of the VFTs, while a second and more compact arrangement involves a larger interface. Cryo-electron microscopy analyses confirm that both arrangements could be detected for the same iGluR and may correspond to different states of the channel (Herguedas et al., 2016). We hypothesized that the oligomeric $GABA_B$ interaction at the VFT level may mimic the less compact form of iGluR VFTs with $GABA_{B1}$ VFTs constituting the central core and $GABA_{B2}$ VFTs being further apart. Accordingly, we mutated residues in the loop that may be part of the interface and that is poorly conserved in VFT proteins. We showed here that mutating $GABA_{B1}$ in this region significantly altered $GABA_{B1}$-$GABA_{B1}$ interaction at low as well as at high expression levels, as evidenced by the lower TR-FRET signal between the N-terminal SNAP tags. Since the ligand affinity was not altered by the mutations, it is unlikely that the folding of the VFT is modified but rather that the general organization of the oligomer is altered. Of note, the fluorophore pair that is used in this study is not sensitive to the dipole orientation such that the TR-FRET signal is dependent mainly on the distance between the fluorophores, and also on the proportion of fluorophores involved in FRET. Our observation that the mutations decreases the TR-FRET signal measured between $GABA_{B1}$ VFTs to values that are still higher than the negative control indicates that the mutations affect the oligomer organization but do not fully prevent the interaction between $GABA_B$ heterodimers. This is further supported by co-immunoprecipitation experiments indicating that even in the presence of the N380 + T382 mutation, $GABA_B$ oligomers could still be detected. It is therefore likely that the mutations affect the mode of interaction between the VFTs, leading to a decrease in affinity of the $GABA_{B1}$ subunit for itself

most probably resulting in a lower proportion of $GABA_B$ oligomers, consistent with the decrease in TR-FRET signal. Altogether, our data bring strong evidence for i) the poorly conserved loop encompassing the residues Glu380 and Leu382 directly participating in the VFT oligomerization interface and ii) the existence of other molecular determinants, likely in the 7TM, in the oligomeric interface. To gain better knowledge of the molecular organization of the $GABA_B$ receptor oligomers, more work is needed, and clearly the determination of the structure of the VFT tetramer would be important.

No matter the exact mode of association of the $GABA_{B1}$ subunits, it is clear that the N380 + T382 mutation affects the allosteric interaction between the $GABA_B$ receptor heterodimers in the oligomer. We previously reported that expression of competing inactive $GABA_{B1}$ subunits that prevents the formation of $GABA_B$ oligomers almost doubles the receptor coupling efficacy to a chimeric PLC activating G protein (Comps-Agrar et al., 2011). Although such an effect could be the consequence of allosteric interaction between the competitor and the functional heterodimer, our observation that mutations at a possible $GABA_{B1}$ VFT dimer interface had the same effect, was in favor of a negative functional cooperativity between the $GABA_B$ heterodimers. In the present study we confirm that it is indeed the case even when examining the coupling of the N380 + T382 mutant to its natural pathway involving Gi proteins with about twice the maximal response of wild-type oligomers. Such a finding suggests that an allosteric interaction between the $GABA_{B1}$ VFTs within the oligomer is essential to control Gi protein coupling efficacy, and that the NT mutation suppresses this allosteric interaction even without fully preventing oligomer formation.

The existence of allosteric interaction between VTFs is further clearly demonstrated when analyzing the binding properties of the fluorescent ligand CGP54626-Red, revealing that the apparent number of binding sites is almost double when using $GABA_{B1}$-NT compared to the wild-type subunit, without any significant change in affinity. This indicates that in average, for an equivalent number of $GABA_B$ heterodimers, fewer CGP54626 molecules bind to the oligomer and that destabilizing their molecular organization results in an increase in the number of bound antagonists. In other words, this strongly suggests that the mutation leads to steric hindrance or disruption of subtle molecular switches that prevent the simultaneous occupancy of all the binding sites by the orthosteric antagonist and then reveals a strong negative allostery within the oligomer. This is well demonstrated by the lack of LRET between CGP54626 labeled with a donor and an acceptor. Moreover, because LRET can be measured between $GABA_{B1}$ VFT N-termini, and because the orthosteric binding site is in the $GABA_{B1}$ VFT (Galvez et al., 2000), the distance between binding sites is likely to be compatible with LRET. Altogether, this supports a strong negative allostery for antagonist binding within the oligomers such that, at the equilibrium, only a fraction of the sites can be occupied.

Does the negative allostery also apply to agonists? So far, we do not have access to a fluorescent or a radioactive agonist with a high enough affinity to reproduce the experiments performed with the antagonist. However, we may hypothesize that the negative allostery is also likely for agonists. Indeed, the reduced efficacy in G protein activation by agonists in intact versus destabilized oligomers may directly reflect the occupancy of binding sites. We have previously shown in mGlu receptors, that two agonists are more efficient in G protein activation compared to a single ligand-bound dimer (Kniazeff et al., 2004). In addition, we had previously set up conditions that

allowed insertion of a GABA binding deficient heterodimers in the oligomers (Comps-Agrar et al., 2011). This similarly resulted in an increase in G protein coupling efficacy. Altogether, these observations support the existence of a negative allostery between orthosteric binding site within the $GABA_B$ receptor oligomers for both agonist and antagonist binding. Such finding provides a rational explanation for the proposed hypothesis that only one heterodimer is functional in a tetrameric element of the $GABA_B$ oligomer.

What would be the physiological significance of having $GABA_B$ receptor oligomers activating a limited number of G proteins compared to heterodimers all activating a G protein (Figure 5)? We could speculate that, *in vivo*, an equilibrium exists between oligomers and heterodimers such that oligomers constitute a storage pool of receptors that could be dissociated to increase the strength of the $GABA_B$ receptor response under some physiological contexts. Indeed, $GABA_B$ receptor is modulating the synaptic transmission throughout the brain and such a mechanism may prove to be important to protect the brain under certain circumstances. Additionally, the $GABA_B$ receptor oligomers could have some additional and still unknown signaling signatures by modulation other intracellular pathways that are not modulated by the heterodimers. Oligomers may also constitute signaling platforms with interacting proteins bound to the 'inactive' heterodimers placing them in spatial proximity to the 'active' heterodimers to modulate the signaling cascades. All these hypotheses are still very speculative but there are nonetheless compelling avenues which to address in a physiological context to decipher the role of the $GABA_B$ receptor oligomers *in vivo*.

Abbreviations

GPCR: G protein-coupled receptor; mGluR: metabotropic glutamate receptor; VFT: venus flytrap; 7TM: seven transmembrane domain; LRET: Lanthanide resonance energy transfer; TR-FRET: Time resolved Förster resonance energy transfer; ER: endoplasmic reticulum; PLC: phospholipase C; ST: Snap-tag; IP: immunoprecipitation; BRET: bioluminescence resonance energy transfer; iGluR: ionotropic glutamate receptor.

Fundings

This work has been supported by ANR grants grants from the French Ministry of Research, Agence Nationale de la Recherche (ANR-09-BLAN-0272; ANR-12-BSV2-0015). G.S. was supported by a postdoctoral fellowship from the Fondation pour la Recherche Médicale; L.C.-A. was supported by a Conventions Industrielles de Formation par la Recherche fellowship from Cisbio Bioassays and the French government. L.N.-L. was supported by grants from the Faculty of Pharmaceutical Sciences, University of Copenhagen "FARMA puljen", from Forsikringsforeningen for farmaceuter i Danmark, "FFF-puljen" and from Danske Bank studielegat.

Declaration of interest

The authors declare no conflicts of interest.

Acknowledgments

We would like to thank Jordan Sinnes and Priscylia Cholot for technical assistance. The fluorescence measurements were performed at the ARPEGE (Pharmacology, Screening, Interactome) facility at the Institut de Génomique Fonctionnelle.

References

Bettler, B., Kaupmann, K., Mosbacher, J., Gassmann, M., 2004. Molecular structure and physiological functions of GABA(B) receptors. Physiol Rev 84, 835-867.

Bowery, N. G., Bettler, B., Froestl, W., Gallagher, J. P., Marshall, F., Raiteri, M., Bonner, T. I., Enna, S. J., 2002. International Union of Pharmacology. XXXIII. Mammalian gamma-aminobutyric acid(B) receptors: structure and function. Pharmacol Rev 54, 247-264.

Burmakina, S., Geng, Y., Chen, Y., Fan, Q. R., 2014. Heterodimeric coiled-coil interactions of human GABAB receptor. Proc Natl Acad Sci U S A 111, 6958-6963.

Calebiro, D., Rieken, F., Wagner, J., Sungkaworn, T., Zabel, U., Borzi, A., Cocucci, E., Zurn, A., Lohse, M. J., 2013. Single-molecule analysis of fluorescently labeled G-protein-coupled receptors reveals complexes with distinct dynamics and organization. Proc Natl Acad Sci U S A 110, 743-748.

Calver, A. R., Robbins, M. J., Cosio, C., Rice, S. Q., Babbs, A. J., Hirst, W. D., Boyfield, I., Wood, M. D., Russell, R. B., Price, G. W., Couve, A., Moss, S. J., Pangalos, M. N., 2001. The C-terminal domains of the GABA(b) receptor subunits mediate intracellular trafficking but are not required for receptor signaling. J Neurosci 21, 1203-1210.

Comps-Agrar, L., Kniazeff, J., Norskov-Lauritsen, L., Maurel, D., Gassmann, M., Gregor, N., Prezeau, L., Bettler, B., Durroux, T., Trinquet, E., Pin, J. P., 2011. The oligomeric state sets GABA(B) receptor signalling efficacy. EMBO J 30, 2336-2349.

Cryan, J. F., Kaupmann, K., 2005. Don't worry 'B' happy!: a role for GABA(B) receptors in anxiety and depression. Trends Pharmacol Sci 26, 36-43.

Doumazane, E., Scholler, P., Zwier, J. M., Trinquet, E., Rondard, P., Pin, J. P., 2011. A new approach to analyze cell surface protein complexes reveals specific heterodimeric metabotropic glutamate receptors. FASEB J 25, 66-77.

Filip, M., Frankowska, M., Sadakierska-Chudy, A., Suder, A., Szumiec, L., Mierzejewski, P., Bienkowski, P., Przegalinski, E., Cryan, J. F., 2015. GABAB receptors as a therapeutic strategy in substance use disorders: focus on positive allosteric modulators. Neuropharmacology 88, 36-47.

Galvez, T., Duthey, B., Kniazeff, J., Blahos, J., Rovelli, G., Bettler, B., Prezeau, L., Pin, J. P., 2001. Allosteric interactions between GB1 and GB2 subunits are required for optimal GABA(B) receptor function. EMBO J 20, 2152-2159.

Galvez, T., Prezeau, L., Milioti, G., Franek, M., Joly, C., Froestl, W., Bettler, B., Bertrand, H. O., Blahos, J., Pin, J. P., 2000. Mapping the agonist-binding site of GABAB type 1 subunit sheds light on the activation process of GABAB receptors. J Biol Chem 275, 41166-41174.

Geng, Y., Bush, M., Mosyak, L., Wang, F., Fan, Q. R., 2013. Structural mechanism of ligand activation in human GABA(B) receptor. Nature 504, 254-259.

Herguedas, B., Garcia-Nafria, J., Cais, O., Fernandez-Leiro, R., Krieger, J., Ho, H., Greger, I. H., 2016. Structure and organization of heteromeric AMPA-type glutamate receptors. Science 352, aad3873.

Jiang, L. I., Collins, J., Davis, R., Lin, K. M., DeCamp, D., Roach, T., Hsueh, R., Rebres, R. A., Ross, E. M., Taussig, R., Fraser, I., Sternweis, P. C., 2007. Use of a cAMP BRET sensor to characterize a novel regulation of cAMP by the sphingosine 1-phosphate/G13 pathway. J Biol Chem 282, 10576-10584.

Jones, K. A., Borowsky, B., Tamm, J. A., Craig, D. A., Durkin, M. M., Dai, M., Yao, W. J., Johnson, M., Gunwaldsen, C., Huang, L. Y., Tang, C., Shen, Q., Salon, J. A., Morse, K., Laz, T., Smith, K. E., Nagarathnam, D., Noble, S. A., Branchek, T. A., Gerald, C., 1998. GABA(B) receptors function as a heteromeric assembly of the subunits GABA(B)R1 and GABA(B)R2. Nature 396, 674-679.

Kammerer, R. A., Frank, S., Schulthess, T., Landwehr, R., Lustig, A., Engel, J., 1999. Heterodimerization of a functional GABAB receptor is mediated by parallel coiled-coil alpha-helices. Biochemistry 38, 13263-13269.

Kaupmann, K., Malitschek, B., Schuler, V., Heid, J., Froestl, W., Beck, P., Mosbacher, J., Bischoff, S., Kulik, A., Shigemoto, R., Karschin, A., Bettler, B., 1998. GABA(B)-receptor subtypes assemble into functional heteromeric complexes. Nature 396, 683-687.

Kniazeff, J., Bessis, A. S., Maurel, D., Ansanay, H., Prezeau, L., Pin, J. P., 2004. Closed state of both binding domains of homodimeric mGlu receptors is required for full activity. Nat Struct Mol Biol 11, 706-713.

Kniazeff, J., Prezeau, L., Rondard, P., Pin, J. P., Goudet, C., 2011. Dimers and beyond: The functional puzzles of class C GPCRs. Pharmacol Ther 130, 9-25.

Kuner, R., Kohr, G., Grunewald, S., Eisenhardt, G., Bach, A., Kornau, H. C., 1999. Role of heteromer formation in GABAB receptor function. Science 283, 74-77.

Lee, C. H., Lu, W., Michel, J. C., Goehring, A., Du, J., Song, X., Gouaux, E., 2014. NMDA receptor structures reveal subunit arrangement and pore architecture. Nature 511, 191-197.

Margeta-Mitrovic, M., Jan, Y. N., Jan, L. Y., 2000. A trafficking checkpoint controls GABA(B) receptor heterodimerization. Neuron 27, 97-106.

Maurel, D., Comps-Agrar, L., Brock, C., Rives, M. L., Bourrier, E., Ayoub, M. A., Bazin, H., Tinel, N., Durroux, T., Prezeau, L., Trinquet, E., Pin, J. P., 2008. Cell-surface protein-protein interaction analysis with time-resolved FRET and snap-tag technologies: application to GPCR oligomerization. Nat Methods 5, 561-567.

Maurel, D., Kniazeff, J., Mathis, G., Trinquet, E., Pin, J. P., Ansanay, H., 2004. Cell surface detection of membrane protein interaction with homogeneous time-resolved fluorescence resonance energy transfer technology. Anal Biochem 329, 253-262.

Pagano, A., Rovelli, G., Mosbacher, J., Lohmann, T., Duthey, B., Stauffer, D., Ristig, D., Schuler, V., Meigel, I., Lampert, C., Stein, T., Prezeau, L., Blahos, J., Pin, J., Froestl, W., Kuhn, R., Heid, J., Kaupmann, K., Bettler, B., 2001. C-terminal interaction is essential for surface trafficking but not for heteromeric assembly of GABA(b) receptors. J Neurosci 21, 1189-1202.

Schwenk, J., Metz, M., Zolles, G., Turecek, R., Fritzius, T., Bildl, W., Tarusawa, E., Kulik, A., Unger, A., Ivankova, K., Seddik, R., Tiao, J. Y., Rajalu, M., Trojanova, J., Rohde, V., Gassmann, M., Schulte, U., Fakler, B., Bettler, B., 2010. Native GABA(B) receptors are heteromultimers with a family of auxiliary subunits. Nature 465, 231-235.

Sobolevsky, A. I., Rosconi, M. P., Gouaux, E., 2009. X-ray structure, symmetry and mechanism of an AMPA-subtype glutamate receptor. Nature 462, 745-756.

Ulrich, D., Bettler, B., 2007. GABA(B) receptors: synaptic functions and mechanisms of diversity. Curr Opin Neurobiol 17, 298-303.

White, J. H., Wise, A., Main, M. J., Green, A., Fraser, N. J., Disney, G. H., Barnes, A. A., Emson, P., Foord, S. M., Marshall, F. H., 1998. Heterodimerization is required for the formation of a functional GABA(B) receptor. Nature 396, 679-682.

Zhu, S., Stein, R. A., Yoshioka, C., Lee, C. H., Goehring, A., McHaourab, H. S., Gouaux, E., 2016. Mechanism of NMDA Receptor Inhibition and Activation. Cell 165, 704-714.

Figure Legends

Figure 1: $GABA_B$ receptor oligomerization and destabilization by N380+T382 mutation. A. Schematic representation of the $GABA_B$ receptor subunits, the SNAP-Tag (ST) and the N380+T382 (NT) mutation. B. $GABA_B$ receptors structure where the mutated residues positions are highlighted by colored spheres: 380 and 382 (orange); 410 and 412 (green) and 413 (purple) ($GABA_{B1a}$ numbering). $GABA_{B1}$ subunit is represented in grey, $GABA_{B2}$ subunit in black. The image was generated using pymol. The pdb code for the $GABA_B$ VFT dimer structure is 4MQE. C. Measurement of TR-FRET signal between $GABA_B$ receptor subunits over a large range of cell surface expression. HEK293 cells were transfected with ST-$GABA_{B1}$ and $GABA_{B2}$ (black), ST-$GABA_{B1}$-NT and $GABA_{B2}$ (orange) or $GABA_{B1}$ and ST-$GABA_{B2}$ (blue) and labeled either with an optimized amount of the SNAP-Lumi4Tb (donor) and SNAP-Red (acceptor) for TR-FRET signal recording or with a saturating concentration of SNAP-Lumi4Tb for determination of cell surface expression. Both the TR-FRET signal and cell surface expression were determined and plotted (data points from 4 independent experiments each performed in three replicates). D. Co-immunoprecipitation of $GABA_B$ receptor oligomers. HEK293 cells were transfected with cDNA encoding the indicated proteins. After immunoprecipitation using an anti-Flag antibody, HA-tagged proteins were detected by western blot using an anti-HA antibody. Total expression of HA-tagged protein was also assessed. (Gels are representative of 3 independent experiments).

Figure 2: Measurement of intracellular cAMP level upon $GABA_B$ receptor activation using a BRET-based EPAC sensor. Increasing concentrations of GABA were applied

to HEK293 cells expressing either $GABA_{B1}$ and $GABA_{B2}$ (black) or $GABA_{B1}$-NT and $GABA_{B2}$ (orange) and Camyel cAMP sensor and the resulting BRET signal was recorded. The signal is expressed as a percentage of the wild-type receptor response and each data point is the average of three independent experiments ± S.E.M., where each experiment was performed in duplicate.

Figure 3: Binding properties of wild-type or N380+T382 $GABA_B$ receptors using fluorescent orthosteric antagonist CGP54626-Red. A. Competition binding with GABA and CGP54626. Increasing concentrations of GABA (circle) or unlabeled CGP54626 (triangle) were applied to HEK293 cells expressing $GABA_{B1}$ and $GABA_{B2}$ (black) or $GABA_{B1}$-NT and $GABA_{B2}$ (orange) in the presence of 10 nM of Red-CGP54626. The signal is expressed as a percentage of initial binding and each data point is the average of three independent experiments ± S.D., each performed in triplicate. B. Saturation binding of GCP54626-Red. Increasing concentrations of CGP54626-Red were applied to HEK293 cells expressing $GABA_{B1}$ and $GABA_{B2}$ (black) or $GABA_{B1}$-NT and $GABA_{B2}$ (orange). Inset: $GABA_B$ cell surface expression measured by ELISA against N-terminal HA-tagged $GABA_{B1}$. Each data point is the average of three independent experiments ± S.D., each performed in triplicate.

Figure 4: Measurement of fluorescence intensities and TR-FRET signals on $GABA_B$ expressing cells labeled with fluorescent antagonists and/or ST substrates. A. Detection of fluorescent antagonist binding to the $GABA_B$ receptor. Increasing concentrations of CGP54626-Red were applied with 10 nM of CGP54626-Lumi4Tb to HEK293 cells expressing $GABA_{B1}$ and $GABA_{B2}$. The bound compounds were detected by fluorescence at 620 nm (Lumi4Tb – dark purple) or at 670 nM (Red –

dark Red). Data are expressed as a percentage of maximal specific binding. B. Measurement of TR-FRET intensity on the same cells and similar conditions as in A. Data are from a representative experiment performed 3 independent times in triplicate. C. Comparison of TR-FRET signals measured using different combinations of ST and/or antagonist labeling. HEK293 cells expressing $GABA_{B1}$ and ST-$GABA_{B2}$ (left part) or ST-$GABA_{B1}$ and $GABA_{B2}$ (right part) were incubated either with optimized concentrations of indicated SNAP or CGP54626 fluorescent compounds. Data are from a representative experiment performed 3 independent times in triplicate.

Figure 5: Proposed model for ligand binding and G protein activation of different $GABA_B$ receptor oligomeric organizations. $GABA_{B1}$ (light grey) and $GABA_{B2}$ (dark grey) assemble into oligomers (a tetramer is highlighted). Orthosteric ligand binding (blue) is limited in intact oligomers (left) compared to isolated heterodimer (middle) or destabilized oligomers (right). In parallel, G protein (purple) activation is also different depending on the organization of the $GABA_B$ receptor oligomers. This indicates negative allostery (red) within the oligomers.

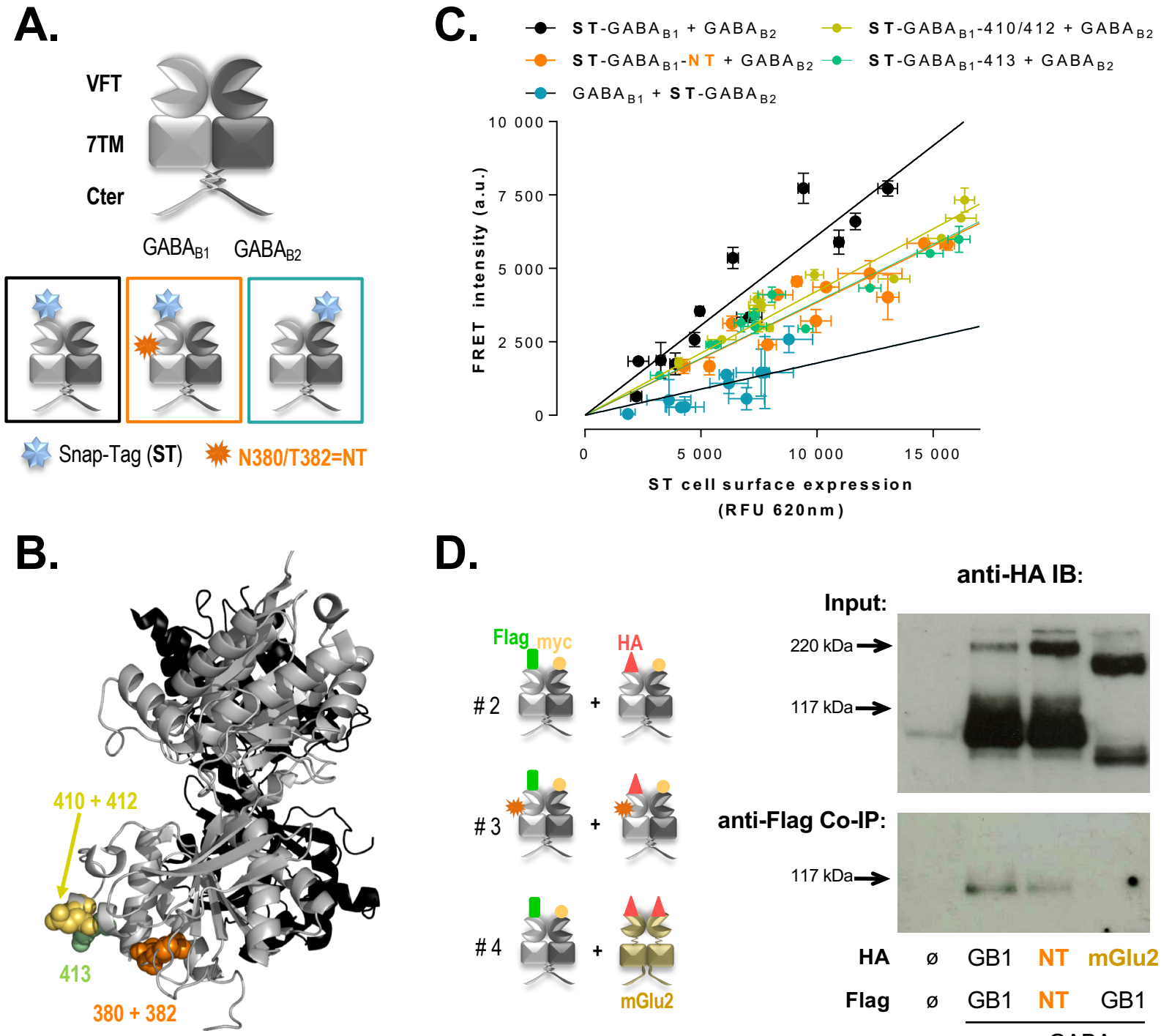
A.
VFT
7TM
Cter
GABA$_{B1}$
GABA$_{B2}$
Snap-Tag (ST)
N380/T382=NT
B.
410 + 412
413
380 + 382
C.
ST-GABA$_{B1}$ + GABA$_{B2}$
ST-GABA$_{B1}$-NT + GABA$_{B2}$
GABA$_{B1}$ + ST-GABA$_{B2}$
ST-GABA$_{B1}$-410/412 + GABA$_{B2}$
ST-GABA$_{B1}$-413 + GABA$_{B2}$
FRET intensity (a.u.)
10 000
7 500
5 000
2 500
0
0
5 000
10 000
15 000
ST cell surface expression
(RFU 620nm)
D.
Flag
myc
HA
#2
#3
#4
mGlu2
anti-HA IB:
Input:
220 kDa
117 kDa
anti-Flag Co-IP:
117 kDa
HA ø GB1 NT mGlu2
Flag ø GB1 NT GB1
+ myc-GABA$_{B2}$
#2 #3 #4

Figure 1

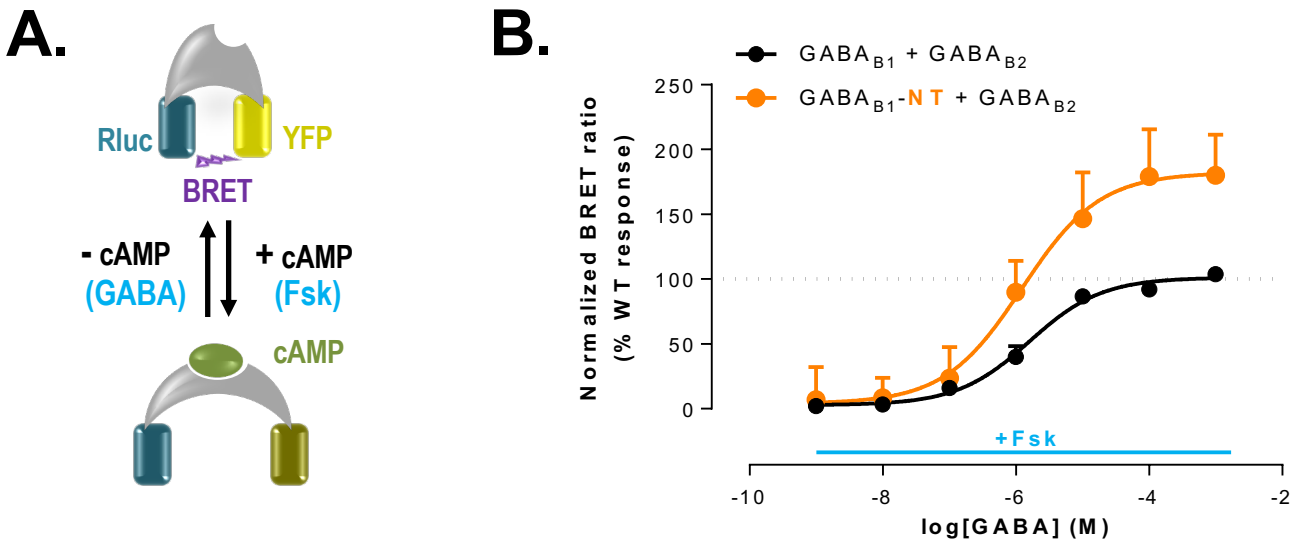
A.
Rluc
YFP
BRET
- cAMP
(GABA)
+ cAMP
(Fsk)
cAMP
B.
GABA$_{B1}$ + GABA$_{B2}$
GABA$_{B1}$-NT + GABA$_{B2}$
Normalized BRET ratio
(% WT response)
250
200
150
100
50
0
+Fsk
-10
-8
-6
-4
-2
log[GABA] (M)

Figure 2

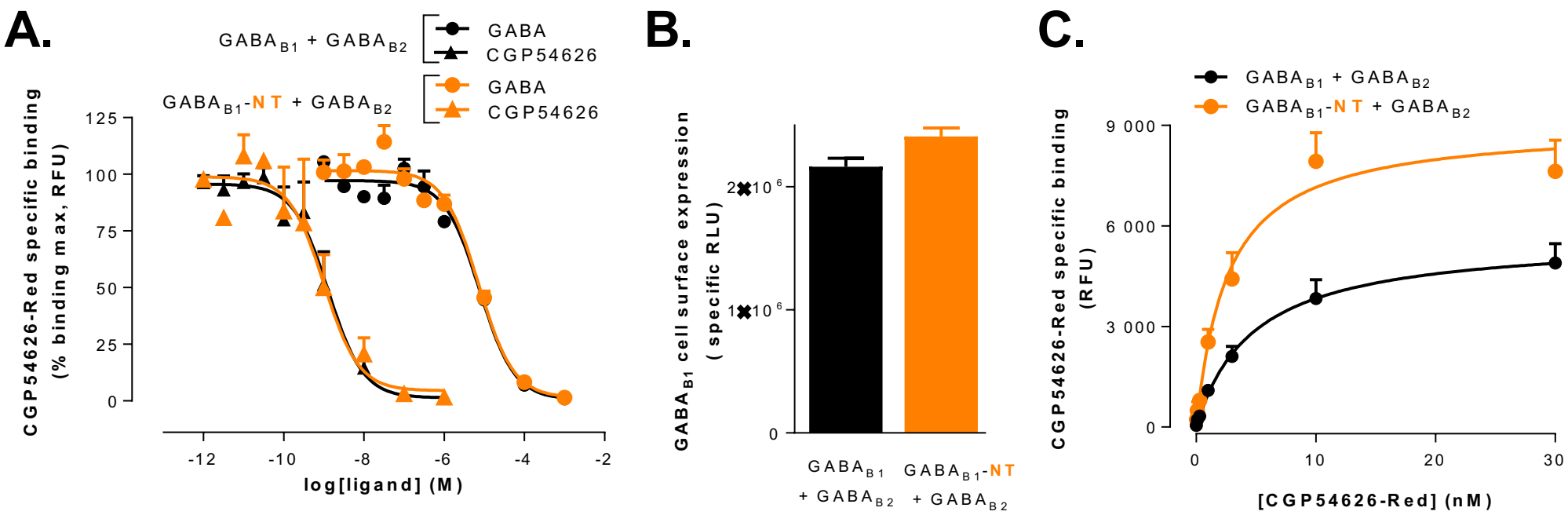
A.
GABA$_{B1}$ + GABA$_{B2}$
GABA
CGP54626
GABA$_{B1}$-NT + GABA$_{B2}$
GABA
CGP54626
CGP54626-Red specific binding
(% binding max, RFU)
125
100
75
50
25
0
-12
-10
-8
-6
-4
-2
log[ligand] (M)
B.
GABA$_{B1}$ cell surface expression
(specific RLU)
2x10^6
1x10^6
0
GABA$_{B1}$ + GABA$_{B2}$
GABA$_{B1}$-NT + GABA$_{B2}$
C.
GABA$_{B1}$ + GABA$_{B2}$
GABA$_{B1}$-NT + GABA$_{B2}$
CGP54626-Red specific binding
(RFU)
9 000
6 000
3 000
0
0
10
20
30
[CGP54626-Red] (nM)

Figure 3

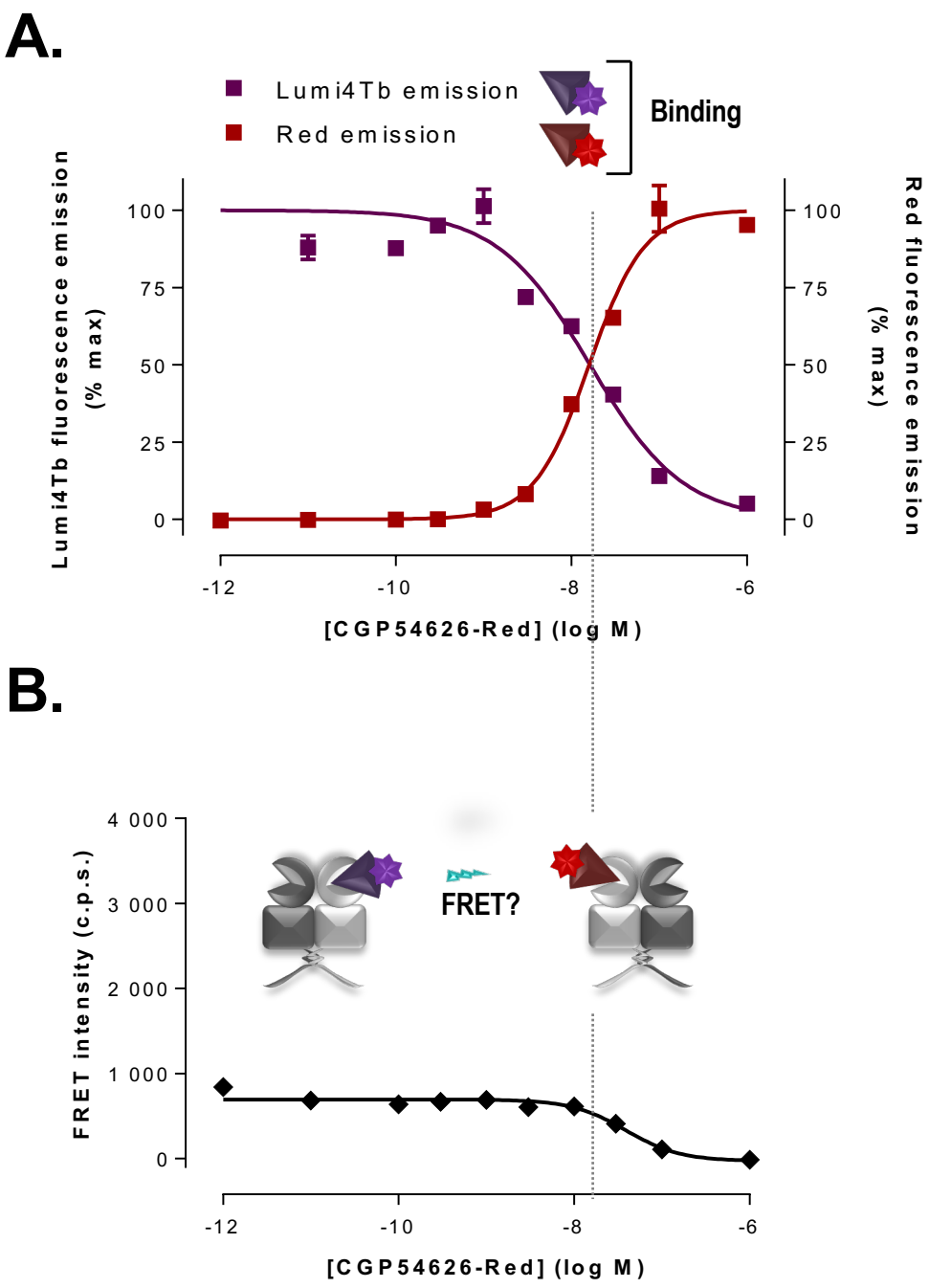
A.
Lumi4Tb emission
Red emission
Binding
Lumi4Tb fluorescence emission (% max)
Red fluorescence emission (% max)
100
75
50
25
0
-12
-10
-8
-6
[CGP54626-Red] (log M)
B.
FRET?
FRET intensity (c.p.s.)
4 000
3 000
2 000
1 000
0
-12
-10
-8
-6
[CGP54626-Red] (log M)
C.
SNAPLumi4Tb + SNAP Red
SNAP Red + CGP54626-Lumi4Tb
CGP54626-Lumi4Tb + CGP54626-Red
FRET intensity (c.p.s.)
3 000
2 000
1 000
0
GABA B1 + ST-GABA B2
ST-GABA B1 + GABA B2

Figure 4

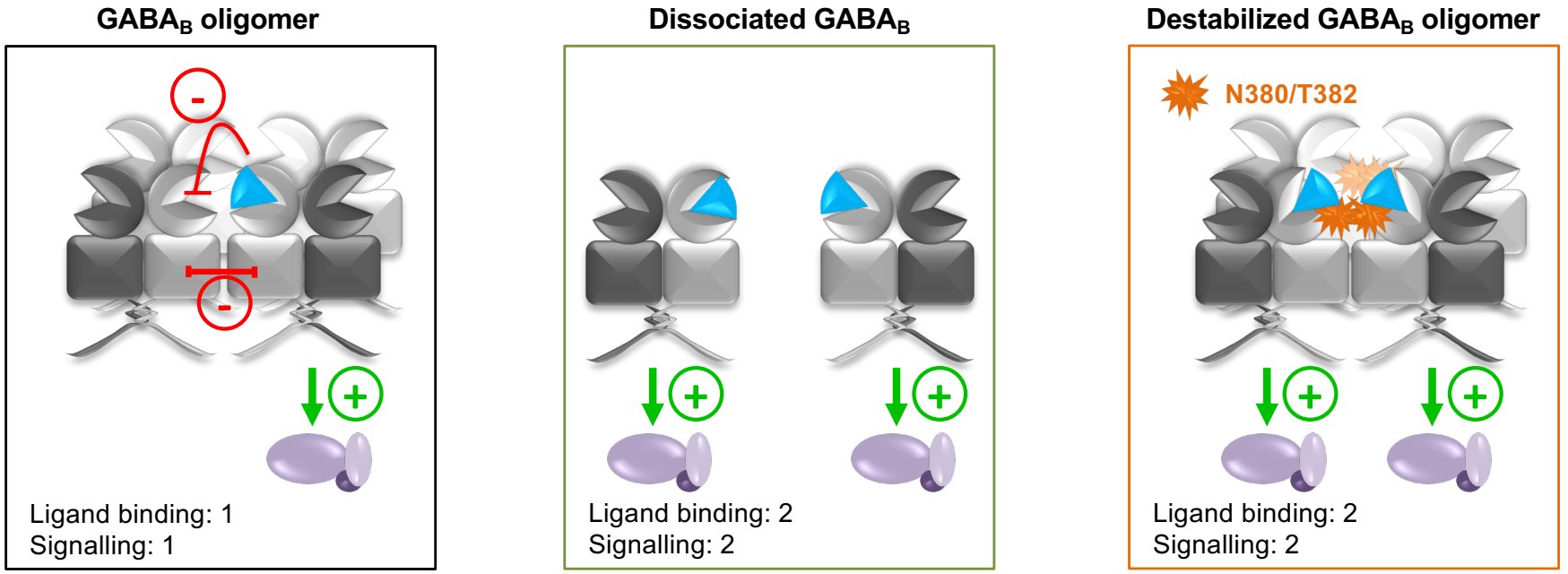
GABA$_B$ oligomer
Ligand binding: 1
Signalling: 1
Dissociated GABA$_B$
Ligand binding: 2
Signalling: 2
Destabilized GABA$_B$ oligomer
N380/T382
Ligand binding: 2
Signalling: 2

Figure 5

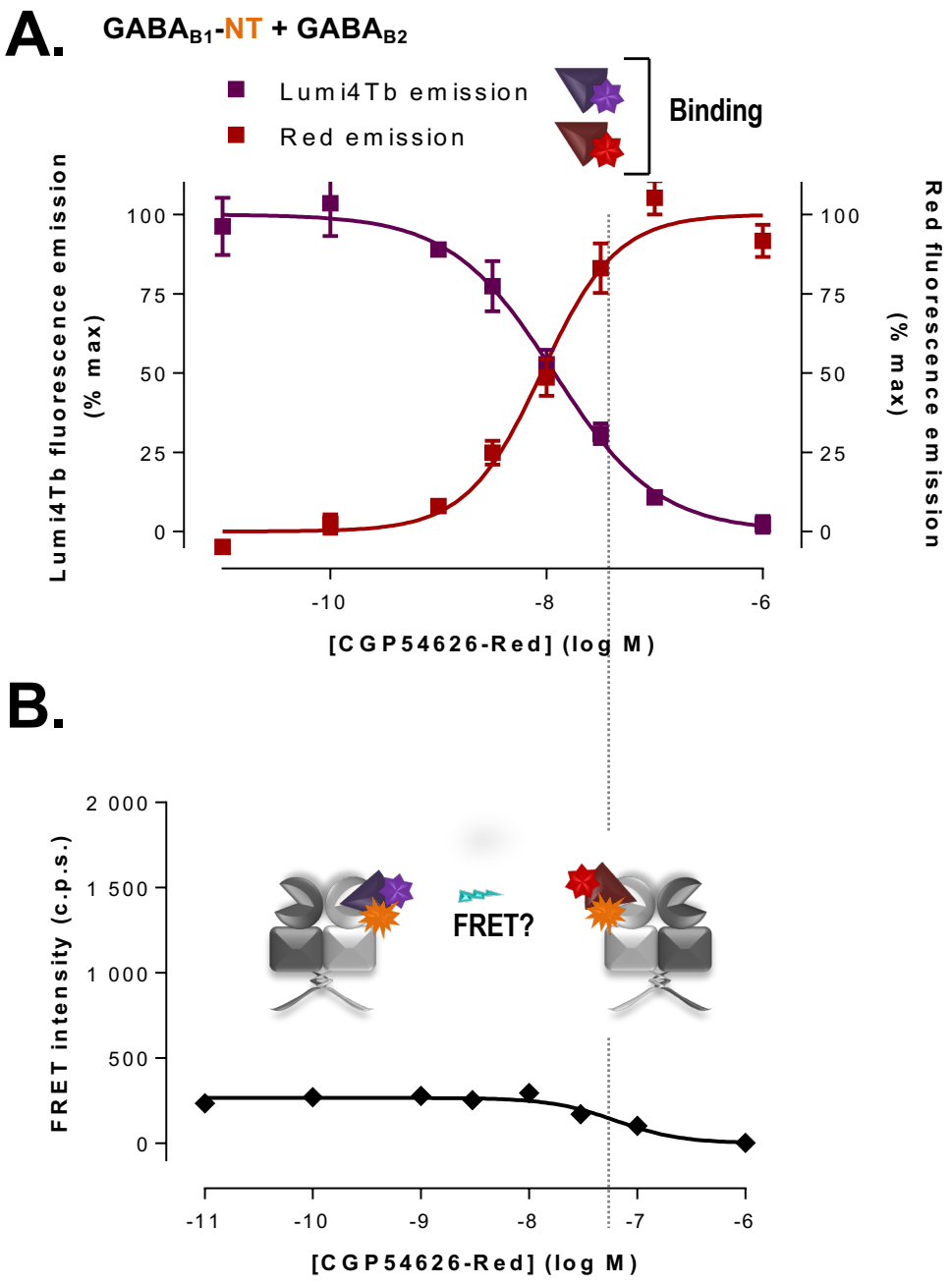

Supp Figure 1 Measurement of fluorescence intensities and TR-FRET signals on cells transfected with GABA$_{B1}$-Mut and GABA$_{B2}$ and labeled with fluorescent antagonists. A. Detection of fluorescent antagonist binding to the GABA$_B$ receptor. Increasing concentrations of CGP54626-Red were applied with 10 nM of CGP54626-Lumi4Tb to HEK293 cells expressing GABA$_{B1}$-Mut and GABA$_{B2}$. The bound compounds were detected by fluorescence at 620 nm (Lumi4Tb – dark purple) or at 670 nM (Red – dark Red). Data are expressed as a percentage of maximal specific binding. B. Measurement of TR-FRET intensity on the same cells and similar conditions as in A. Data are from a representative experiment performed 3 independent times in triplicate.

Supp Figure 1